PHASE TIME INVERSION: A SIMPLE METHOD FOR REGIONAL WAVEFORM INVERSION

Charles A. Langston

University of Memphis

Sponsored by National Nuclear Security Administration
Office of Nonproliferation Research and Engineering
Office of Defense Nuclear Nonproliferation

Contract No. DE-FC04-00AL66883

ABSTRACT

Broadband regional waveforms from earthquake and explosion sources contain a wealth of information on crustal and upper mantle velocity structure. Arrival times, amplitudes, and frequency content of individual seismic phases can be affected by many details of structure that include velocity gradient, average velocities, and velocity heterogeneity as well as source type, depth, and time function. Major characteristics of the regional seismogram are also controlled by the simple parameter of receiver distance from the source. Inversion of the regional waveform for source parameters (for use in seismic discrimination) strongly depends on the velocity model assumed and has proven to be a difficult task for broadband seismograms. Typical waveform fitting schemes often employ seismogram differences or correlations that are dominated by the largest amplitude or lowest frequency phases within the wave train such as surface waves. It is difficult to match smaller body-wave-type arrivals or to unravel the interference between phases that traverse many different paths in the structure. Small time differences between observed and synthetic arrivals can thwart the usual methods of waveform matching but are important pieces of data in determining an appropriate velocity model. The "phase time" inversion method utilizes a direct but biased comparison of data and synthetic seismograms to model the arrival time of any phase on the regional seismogram. Phase time differences are incorporated into a stable generalized inverse to obtain earth structure parameters of "ideal" parameterized velocity structures. The method is used to model a large suite of regional seismograms from an earthquake in Africa to obtain a simple 1-D velocity structure that can explain regional waveforms between 200- and 800-km distance. The "Lg" phase is seen to be composed of high phase velocity, multiple shear waves that propagate throughout the crust. Apparently low Lg group velocities are caused by the kinematic effect of progressive crustal multiples undergoing post-critical reflection at the Moho to produce high phase amplitudes, then cutting out because of the positive crustal velocity gradient.

KEY WORDS: waveform inversion, regional wave propagation, crustal structure, mantle structure, Lg

OBJECTIVE

Regional waveforms are a challenge to understand because they are produced by many different wave propagation mechanisms. Even for 1-D structure these may include, for example, surface wave excitation and propagation, head wave propagation, tunneling (as in the production of S*), post-critical reflection, near-surface site resonances, frequency-dependent attenuation effects, and a variety of wave interference effects caused by source type and source placement in the structure. The problems become compounded when regional seismic structures are allowed to vary in two and three dimensions. The objective of this research is to develop a straightforward method to model regional waveforms to obtain estimates of the earth model that can then be used to infer nuclear-explosion-monitoring-relevant source parameters such as source type and depth. The method developed here, the "phase-time inversion" method, is an intuitive technique for matching observed and calculated waveforms. In principle, it can be applied to determining earth structure in two and three dimensions as well as in the 1-D example shown in this paper, as long as accurate synthetic seismograms can be computed for the structure of interest.

RESEARCH ACCOMPLISHED

We utilize a high-quality waveform data set from earthquakes recorded by the 1994-1995 Tanzania Broadband Experiment (Owens et al 1995) to derive a velocity model of the crust and upper mantle of the Archean age Tanzania craton and surrounding Proterozoic mobile belts (Figure 1) that are presently undergoing rifting. The 1994-1995 Tanzania Broadband Experiment consisted of a 20-station broadband seismic network arranged in a skewed cross pattern across Tanzania (Figure 1) with the Archean Age Tanzania craton being the primary target of the experiment (Owens et al 1995; Nyblade et al 1996). We use the broadband waveforms from the 18 August 1994 Lake Rukwa earthquake to first infer the character of regional wave propagation within the crust and mantle and then to quantify the arrival times and amplitudes from a variety of observed seismic phases to produce a velocity model. The Lake Rukwa event was recorded at teleseismic distance and was the subject of a detailed source study by Zhao et al (1997), who determined its source mechanism, source function, and depth. Because the source parameters are known for this event, it can be used to decipher the regional wave propagation across the network.

An initial model of crustal structure was constructed using results from teleseismic receiver functions and short-period surface wave dispersion analysis performed by Last et al (1997). We constrained upper mantle P and S wave velocities by performing travel-time studies of first arrival Pn waves from other regional events and Sn waves from Rukwa event waveforms. Pn velocity within the network is quite high at 8.2 - 8.5 km/s with the higher velocities found within the craton. Sn velocity, using picks from the Rukwa waveforms, is 4.75 km/s and is consistent with the high average Pn wave velocity (8.3 km/s) in the mantle.

Simply plotting the vertical and radial displacement waveforms in a reduced time section using the average Pn and Sn velocities yields important information on the nature of wave propagation across the network. Figure 1 shows a reduced time section for vertical component arrivals before Sn. Clearly, these phases generally travel at Pn velocities and can be interpreted as Pn, sPn and multiples. Figure 2 shows the S wave train in a reduced time section using the average Sn velocity across the network. There is a remarkable succession of Sn and multiple Sn phases that can be traced across the network.

Identifying each phase in the Rukwa data was a straightforward matter involving calculating theoretical travel-time curves in an ideal crustal model. Travel-time curves were computed for an earth model parameterized with a linear gradient in the crust over a homogeneous mantle (Figure 3). Parameters for this model are given in Table 1. The Rukwa source was located at 25-km depth within the lower half of the crust so that the P waveforms of Figure 1 are dominated by Pn, sPn phases and their multiples. The apparent low-velocity move-out of the later arriving energy in the P waveform data is the beginning of the regional PL wave (Helmberger and Engen, 1980).

Early versions of the final earth model shown in Table 1 were successful in predicting the general behavior of the broadband waveforms when synthetic seismograms were calculated using the Rukwa source parameters. Relative amplitudes and times of the different head waves and crustal multiples were roughly correct showing good similarity between data and synthetic. However, it proved difficult to devise a method to use all the data simultaneously to find an optimum structure model.

Several schemes were attempted to refine the velocity model. Because the wavenumber integration algorithm is computationally intensive (Barker 1984), multi-mode surface wave summation was used initially to construct an accurate synthetic for the S wavetrain (e.g., Harkrider 1964; 1970). Because this is a much faster process (by two orders of magnitude in speed), many more earth models could be tested. We used a normalized cross-correlation function to determine the fit between data and synthetic (e.g, Wallace and Helmberger, 1982). However, the multi-mode summation we used was not appropriate for the P wave part of the wavetrain. Furthermore, it was difficult to fit important, relatively high-frequency pulses in the wavetrains of many records because there were significant time shifts between the data and synthetic pulses when the fit was dominated by the longer period portions of the seismogram.

An attempt was made to calculate wavenumber integration synthetics using a coarse grid search algorithm in the crustal structure parameters to regain the P wavetrain portion of the seismogram. Normalized cross-correlation was then used on specific time windows in the data and synthetics in an attempt to model various individual phases. Again, modest time shifts between data and synthetic arrivals placed these arrivals outside of the

correlation time window even though the pulse shapes were not very different. We also discovered that there were consistent absolute time shifts between the data and synthetic waveforms that were probably due to details in the Rukwa source time function or errors in the origin time. These time shifts compounded the problems with the correlation operator windows. Clearly, the similarity of data and synthetics showed that the basic wave propagation was understandable, yet it was difficult to quantify the earth model using features of the data waveforms.

The regional waveform consists of multiple body waves and surface waves, many of which interfere with each other in complex ways. Whichever way the amplitudes work out, travel times of these waves are straightforward functions of crustal velocity structure and thickness. We noticed that many synthetic seismograms for differing earth models often looked similar with the major differences occurring in arrival time for the various component phases within them. Since these features changed their travel time when model parameters changed, we decided to use these time differences as data in a formal generalized inversion for velocity parameters.

Figure 3 illustrates implementation of the process using vertical component data from station MTOR. The earth model is parameterized as shown at the bottom of the figure as a linear velocity gradient in the crust defined by surface P wave velocity, v_1, a basal P wave velocity, v_2, and crustal Poisson's ratio, σ_c. Crustal thickness, h, is also a parameter. Mantle P and S wave velocities are fixed by the travel-time regression of the Rukwa Pn and Sn data. Using an initial guess for the earth model, a synthetic seismogram is constructed (the "reference model" synthetic in Figure 3) and compared to the original. Note that the source parameters are fixed.

"Phase times" are defined as the arrival time of some easily recognizable peak or trough associated with a particular seismic phase arrival. For example on Figure 3, T_j is associated with the trough of Sn and T_{j+1} with the peak of sSn. Because the reference model is not perfect, corresponding peaks and troughs on the synthetic (T^o_j T^o_{j+1} etc.) do not occur at the same times for these phase time picks.

An iterative inversion problem can be set up to simultaneously solve for a new set of model parameters using the phase time misfits. The phase times for the data waveforms, starting model synthetic, and model perturbation synthetics are all picked manually using an interactive graphical interface (Figure 3). This has both drawbacks and natural efficiencies. Obviously, this process introduces biases in the interpretation of the data and synthetics. A choice is made to fit a particular arrival in the data and it is assumed that wave shape for the arrival does not change appreciably across the synthetics. Picking the wrong phase in the synthetics will create problems since the inversion system will have inconsistent data. Another drawback is that picking the phase time manually introduces some error in the time estimate that will affect estimates of the model parameters. Furthermore, this process is not easily made automatic since each iteration of the system requires picking a new set of phase times for the updated model and perturbation synthetics.

However, fitting the phase times directly is *the* intuitive process that a waveform analyst attempts when fitting data with synthetic seismograms. The phase time itself is just a generalization of ray arrival time applied to some consistent feature of the waveform. Reduction of a highly sampled time series with thousands of points to a few pieces of data is a great economy in setting up the inversion problem. For example we applied this technique to 56 broadband waveforms with ~3000 points each from the Rukwa event. Using only unambiguous picks of phase times between data and synthetics, these ~180,000 data points were reduced to 91 phase time picks. There is also an economy in the computation of synthetic seismograms since synthetics for only 5 different models need to be computed to form the reference synthetic seismogram and the perturbation seismograms. Implicit in the formulation are smoothing constraints imposed by the form of the crustal model. Rather than parameterizing a model with many thin layers, simple "ideal" velocity profiles, like the linear gradient used here, can be investigated. This simplifies the inversion set-up and reduces likely problems in parameter resolution when velocity and thickness parameters of many thin layers in a model trade off with one another. If a more complicated model is needed to fit the data, the model can be made incrementally more complex.

Synthetic tests of the technique worked remarkably well by yielding the correct velocity model in a single iteration. Relatively large perturbations of the earth structure parameters produced stable partial derivatives. The method also worked quite well for single-station synthetic tests. Errors in picking the phase times were found to be a minor problem and did not degrade the model parameter estimates significantly. Picks could be

made to within 0.5 sec for the synthetic data with the model parameter variance being, at most, 0.01 km^2 in crustal thickness. Variance for the other parameters was a little larger than numerical noise levels.

Figure 4 shows a subset of results from applying the phase time inversion to the Rukwa waveform data. Table 1 displays the starting model and final inversion model parameters. The strategy used in picking phases was to use clear, isolated peaks in the vertical waveforms and a few of the tangential waveforms. Phase time picks from the radial waveforms are redundant since they contain the same arrivals as on the vertical components. Because the tangential waveforms were more affected by azimuthal radiation pattern effects in the Rukwa source (SH wave nodes for both up and down going waves sweep through the network), we generally avoided picking details in the tangential waveforms and attributed tangential waveform complexity to the influence of scattering and to the greater effect unknowns in the source mechanism have on amplitudes near wave nodes. We also did not pick phase times from complicated regions of the vertical waveforms where it was obvious that many arrivals were interfering with each other. It was heartening to see after inversion that these complex portions of the seismogram at certain stations improved in fit.

One iteration was required to produce a stable model. Table 1 shows that there were only small changes in the earth structure parameters and origin time needed to improve the alignment of numerous phase picks. A variance of 1 s was assumed for the phase time picks for the estimate of model parameter variance. Figure 3 shows a typical misfit between the data and starting model synthetic.

Returning to Figures 1 and 2, it is apparent that the P and S wave trains at regional distances are dominated by critical reflections and head waves from discrete up- and down-going reflections in the Tanzanian crust. The depth of the Rukwa source and its normal fault mechanism combine to create a succession of discrete Sn-type head waves on vertical and radial components of the S wave train. Figure 2 shows how high-amplitude critical S-wave multiple reflections apparently decay in amplitude with distance as the head wave propagates away from the critical distance. This happens over and over as progressively higher-order multiples pass beyond the critical angle of incidence.

This observation has interesting implications for the propagation mechanism for the higher frequency "Lg" phase. Lg is a phase which is of interest in nuclear explosion monitoring since it often travels great distances in the crustal waveguide, is the largest phase seen in high-frequency regional seismograms, and can be used to estimate seismic moment and magnitude (e.g., Herrmann and Kijko, 1983; Kennett, 1986; Hanson et al 1990; Campillo 1990). The study of Lg has an extensive literature, but its propagation mechanism has been difficult to understand because of unknowns in crustal structure and use of relatively limited, single-station data sets.

In the Rukwa data Lg is a high-amplitude S phase with a velocity indicative of the upper crust, here at 3.5 km/s. If the empirical travel-time curve is superimposed on the travel-time curves for multiple S waves, we see that the beginning of Lg is composed of post-critical Moho reflections with later portions of Lg composed of higher order post-critical Moho reflections. Phase velocity for these post-critical reflections is high, being ~4.2 km/s, since they have near-grazing incidence angles at the Moho. This explanation reinforces empirical array studies of the Lg phase performed by Vogfjord and Langston (1990; 1996) using high-frequency data from the Norwegian seismic arrays. Using array beams, they decomposed the Lg wave field to show that low group velocity Lg waves were composed of high phase velocity turning waves and post-critical reflections within the Scandinavian crust.

CONCLUSIONS AND RECOMMENDATIONS

It was possible to derive a crust and mantle velocity model from regional waveform data recorded from the Lake Rukwa earthquake and from first arrival time data picked from other large regional events. The model is very simple, consisting of a crust characterized by a linear velocity gradient over a mantle half-space and is consistent with previous crustal structure studies in the area. The crust and mantle velocity structure of the Tanzania craton is similar to velocity structure in other Archean cratonic areas in that it has high average crustal velocities, high velocities near the Moho, and relatively high upper mantle velocities.

A simple, intuitive method for inverting large data sets of regional waveform data has been developed and is called "phase time" inversion. This method minimizes the misfit between the arrival times of discrete phases on observed and synthetic seismograms. It is similar to tomographic methods except that there is no reliance on ray travel times or explicit formulations of ray geometry. Any seismic phase can be used as long as accurate synthetic seismograms can be computed. Application to the Rukwa regional waveform data showed that, in this case, the inversion problem behaved in a linear fashion. Earth models can be parameterized in terms of simple "ideal" systems to minimize the number of model parameters while preserving basic understanding of the wave propagation involved. "Phase time" inversion should be useful in many other studies of broadband waveforms where there is interest in wave propagation mechanisms and determining earth structure parameters.

REFERENCES

Barker, J.S. (1984), A seismological analysis of the May 1980 Mammoth Lakes, California, earthquakes, Ph.D. thesis, Pennsylvania State University, State College, PA.

Campillo, M. (1990), Propagation and attenuation characteristics of the crustal phase Lg, *Pure Appl. Geophys.*, *132*, 1-19.

Hanson, R.A., F. Ringdal, and P.G. Richards (199), The stability of RMS Lg measurements and their potential for accurate estimation of the yields of Soviet underground nuclear explosions, *Bull. Seism. Soc. Am.*, *80*, 2106-2126.

Harkrider, D.G. (1964), Surface waves in multilayered elastic media: I. Rayleigh ad Love waves from buried sources in a multilayered elastic half-space, *Bull. Seism. Soc. Am.*, *54*, 627-679.

Harkrider, D.G. (1970), Surface waves in multilayered elastic media. Part II. Higher mode spectra and spectral ratios from point sources in plane layered earth models, *Bull. Seism. Soc. Am.*, *60*, 1937-1987.

Helmberger, D.V., and G.R. Engen (1980), Modeling the long-period body waves from shallow earthquakes at regional ranges, *Bull. Seism. Soc. Am.*, *70*, 1699-1714.

Herrmann, R., and A. Kijko (1983), Modeling some empirical vertical component Lg relations, *Bull. Seism. Soc. Am.*, *73*, 157-171.

Kennett, B.L.N. (1986), Lg waves and structural boundaries, *Bull. Seism. Soc. Am.*, *76*, 1133-1141.

Last, R.J., A.A. Nyblade, and C.A. Langston (1997), Crustal structure of the East African Plateau from receiver functions and Rayleigh wave phase velocities, *Jour. Geophys. Res.*, *102*, 24,469-24,483.

Nyblade, A.A., C. Birt, C.A. Langston, T.J. Owens, and R.J. Last (1996), Seismic experiment reveals rifting of craton in Tanzania, *EOS Trans. AGU*, *77*, 520-521.

Owens, T.J., A.A. Nyblade, and C.A. Langston (1995), The Tanzania Broadband Experiment, *IRIS News Letter*, *XIV* (1).

Vogfjord, K.S., and C.A. Langston (1990), Analysis of regional events recorded at NORESS, *Bull. Seism. Soc. Am.*, *80*, 2016-2031.

Vogfjord, K.S., and C.A. Langston (1996), Characteristics of short-period wave propagation in regions of Fennoscandia, with emphasis on Lg, *Bull. Seism. Soc. Am.*, *86*, 1873-1895.

Wallace, T.C., and D.V. Helmberger (1982), Determining source parameters of moderate-sized earthquakes from regional waveforms, *Phys. Earth and Planet. Int.*, *30*, 185-196.

Zhao, M., C.A. Langston, A.A. Nyblade, and T.J. Owens (1997), Lower-crustal rifting in the Rukwa Graben, East Africa, *Geophysical Journal International*, *129*, 412-420.

Zhu, L., and D.V. Helmberger (1996), Advancement in source estimation techniques using broadband regional seismograms, *Bull. Seism. Soc. Am.*, *86*, 1634-1641.

Table 1. Inversion Model Parameters

	v_1 (km/s)	v_2 (km/s)	σ_c	h (km)	t_0 (s)
Starting model	5.80	7.00	0.250	38.0	0.0
All stations	5.84±0.04	7.09±0.06	0.250±0.005	40.4±0.6	2.2±0.2

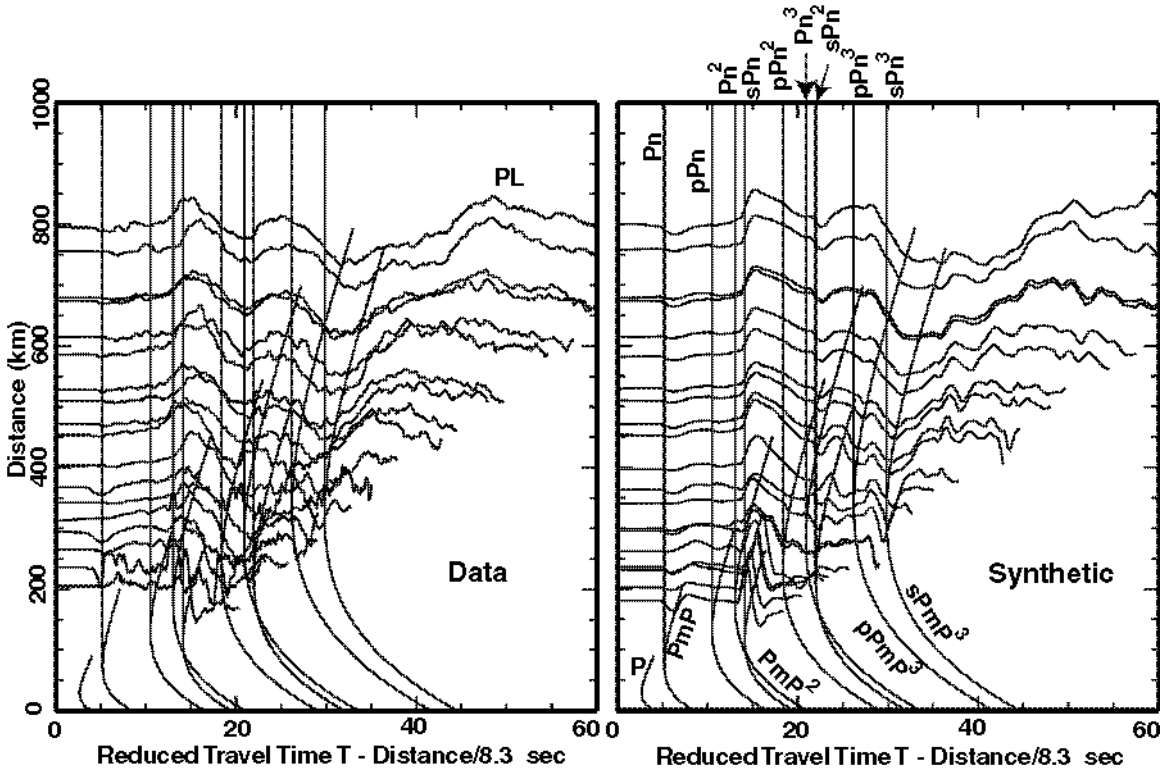

Figure 1. Reduced velocity profiles of vertical displacement data from the Rukwa earthquake and synthetic waveforms from the final inversion model. The data and synthetics have been windowed to exclude the S wavetrain. Note how all waveforms are dominated by waves that travel at Pn velocity. Travel-time curves for major P and sP waves are superimposed on the plot. The largest amplitude phases in the data are sPn-type head waves. Refer to Figure 6 for ray path diagrams. Pn^2 and Sn^2, for example, are mantle head waves associated with PmP^2 and SmS^2 crustal multiples, respectively. All wavenumber synthetic seismograms in this paper were computed using 2048 time points with a 5sps sampling frequency.

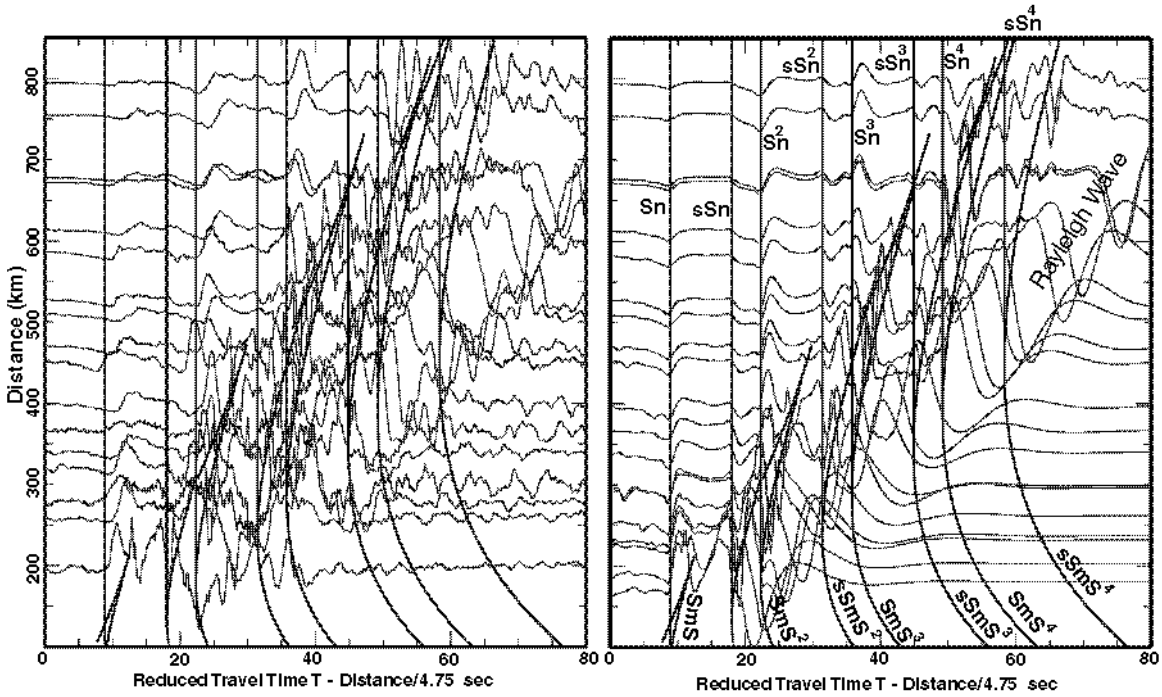

Figure 2. Reduced velocity profiles of vertical displacement data from the Rukwa earthquake and synthetic waveforms from the final inversion model for the S wave train. Travel-time curves for important S wave ray paths are superimposed on the waveform sections. These waveforms contain both Sn-type head waves and post-critical angle multiple S wave reflections.

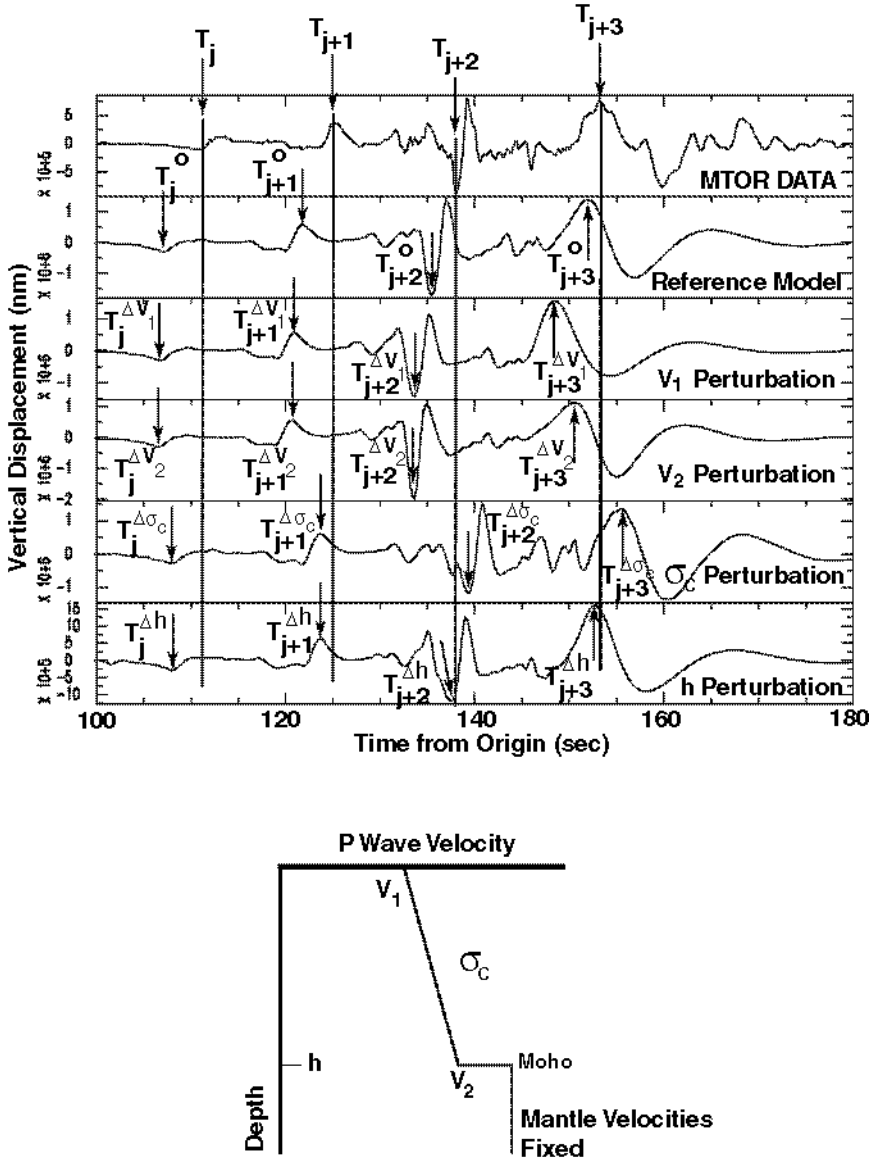

Figure 3. Illustration of picking phase times from observed and synthetic regional waveforms (top panel). Vertical component data from Kwa Mtoro (MTOR) station is shown at the top. A synthetic seismogram is shown just below ("reference model") computed using the starting earth model, and four other synthetics below that are computed using perturbations of the starting earth model. The earth model is parameterized by a linear gradient in the crust over a mantle half-space as shown in the lower panel and arrival times are a function of the assumed source and structure parameters. "Phase times" are picked using obvious peaks or troughs for various arrivals in the data. For example, each phase time shown in the figure corresponds to Sn (T_j), Sn^2 (T_{j+1}), $sSmS^2$ (T_{j+2}), and the Rayleigh wave (T_{j+3}). The corresponding peak or trough is picked on the synthetic waveforms to form the phase time residual and partial derivatives.

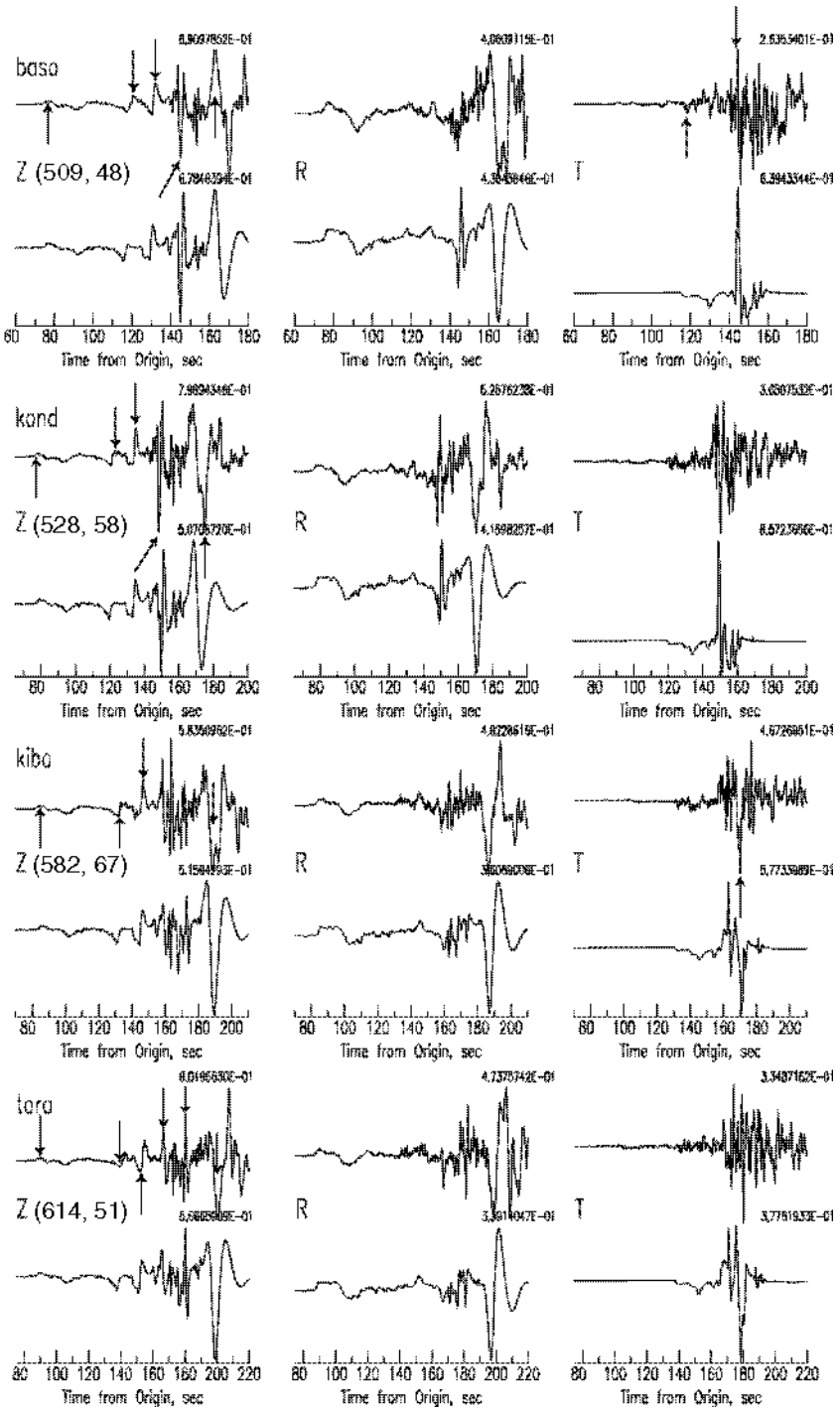

Figure 4. Observed (top) and synthetic (bottom) regional seismograms for the Lake Rukwa earthquake. Vertical (Z), radial (R), and tangential (T) waveforms are shown for each station. Station distance (km) and azimuth from the source (degrees) are shown in parentheses. Seismograms have been normalized for plotting and the absolute amplitude (microns) is given in the upper right of each seismogram. The arrows denote phase time picks used in the inversion. Note that the time scale generally changes with station distance.